INSTITUTE OF PHYSICS PUBLISHING JOURNAL OF PHYSICS: CONDENSED MATTER

J. Phys.: Condens. Matter **13** (2001) 7691–7706 PII: S0953-8984(01)24198-8

Layered magnetic structures: facts, figures, future

P Grünberg[1]

Forschungszentrum Jülich-IFF, 52425 Jülich, Germany

E-mail: p.gruenberg@fz-juelich.de

Received 24 April 2001
Published 9 August 2001
Online at stacks.iop.org/JPhysCM/13/7691

Abstract

An overview is given of the most important properties of layered magnetic structures. This includes the effects of interface anisotropy and exchange bias as well as the magnetic properties of ultrathin films in the monolayer range. The current understanding of interlayer exchange coupling, giant magnetoresistance and tunnel magnetoresistance will also be indicated. Future efforts will most likely include interlayer coupling induced by spin injection. Typical and record values for the strengths of the observed effects are compiled from the literature.

1. First experiments

The first experiment on thin magnetic films was performed by A Kundt in 1884 who proved that there is a rotation of the polarization of light when it propagates through ferromagnetic metals like Fe, Co or Ni [1]. It is clear that thin films were required to do such experiments. Earlier, Faraday had seen this 'Faraday rotation' in a specimen of glass, subject to a magnetic field. For almost a century the investigation of this effect became the main driving force for research in thin magnetic films. Kundt established the proportionality between the rotation and the magnetization component parallel to the light beam. This was called Kundt's law, the proportionality factor being Kundt's constant.

While Kundt used electrochemical deposition for the preparation of his films, due to the improvements in vacuum techniques by 1950 thermal evaporation was favoured which enabled research on a more reliable basis. As a result, in 1968 surface anisotropy (or more generally interface anisotropy) was seen for the first time experimentally [2]; this had already been predicted by Néel in 1954. We turn now to a description of this and other interesting phenomena which have been discovered in layered magnetic structures.

2. Special anisotropies at surfaces and interfaces

Néel-type surface anisotropy is due to the symmetry breaking at a surface and can be predicted from data on bulk anisotropy and magnetostriction. This is not the only possibility [2]. Extended work by various theory groups has established a relation between anisotropy and

[1] Fax: ++49-2461-614443.

spin–orbit coupling and hence more generally with the electronic band structure. On the basis of this, the appearance of strong perpendicular anisotropy in Co/Pd multilayers reported in 1985 was explained theoretically. Since Ni has the same number of valence electrons as Pd, the calculations were extended to Co/Ni structures and it was predicted that a strong interface anisotropy with the easy axis perpendicular to the sample plane should exist also at the Co/Ni interface. Indeed experiments on $(Co1/Ni2)_{20}$ layered structures with a total thickness of 120 Å showed strong perpendicular anisotropy, as predicted, orienting the magnetization spontaneously perpendicular to the sample plane. The result is displayed in figure 1, where the magnetization saturates in small fields applied perpendicular to the sample plane ($\perp$) and in large fields when applied in the plane ($\parallel$).

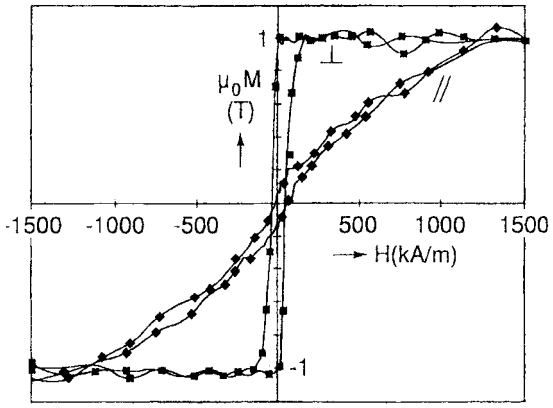

Figure 1. Remagnetization curves of $(Co1/Ni2)_{20}$ layered structures, showing perpendicular anisotropy [2].

Table 1 contains values for the strength of the interface anisotropy as defined by

$$\sigma_i = K_S \cos^2 \theta \tag{1}$$

where σ_i is the areal energy density connected with the anisotropy, and the magnetization includes an angle θ with the surface normal. Equation (1) is a phenomenological expression for the description of the effect. For a negative value of the surface anisotropy constant K_S, minimum energy is obtained for $\theta = 0$ and $\theta = 180^\circ$ and the normal to the sample plane is an easy axis. For positive K_s the easy axis lies in the sample plane.

Table 1. Values for K_S as defined by equation (1), compiled from the literature [2]. The free surface is indicated by 'UHV'.

Interface	K_S (mJ m^{-2})
Co/Pd	−0.92
Co/Pt	−1.15
Co/Ni	−0.42
Co/Au	−1.28
Ni/UHV	0.48
Ni/Cu	0.22
Fe/Ag	−0.79
Fe/Au	−0.54
Fe/UHV	−0.89

The demagnetizing areal energy density, which favours the magnetization being in the sample plane, is $0.5\mu_0 M^2 t$, where M is the magnetization and t the thickness of the film. For a monolayer of Fe with $t = 0.14$ nm we obtain 0.53 mJ m^{-2}. Hence by comparison with the values in table 1 we would expect for example for the Fe/Au system a spontaneous orientation of the magnetization perpendicular to the sample plane only in the limit of one monolayer of Fe. (The corresponding energy for a Fe monolayer due to an external field $B = \mu_0 H = 0.1$ T is $BMt = 0.025$ mJ m^{-2}.)

Apart from choosing the right materials, one can increase the influence of σ_i on the total anisotropy further, by increasing the density of interfaces. This was carried to the extreme of alternating just one monolayer of Fe with one monolayer of Au or Pt in reference [3]. The saturation fields were around 2 T in the case of $(Fe/Au)_{100}$ films and more than 6 T in the case of $(Fe/Pt)_{100}$.

In thin films the electronic properties are characterized by quantum well states. This aspect of the dependence of the surface anisotropy on electronic properties has also recently been demonstrated [4]. The surface anisotropy of a Co film oscillates and even changes sign as a function of the thickness of a Cu overlayer. This is clearly due to the quantum well states in the Cu.

Another type of anisotropy, which can also be classified as interface anisotropy, is the so-called 'exchange bias' [5]. It was first seen in 1956 in fine Co particles covered by antiferromagnetic Co oxide, but soon also reproduced in thin-film structures. By means of this effect it is possible to shift hysteresis curves of samples on the field axis. An example is shown in figure 2 [5, 6] for a so-called 'spin-valve structure'. The 'free' layer remagnetizes in small fields whereas the hysteresis curve of the 'pinned' layer is shifted to positive fields by the 'exchange field' H_E. Part (c) shows the related GMR effect to be discussed below. We

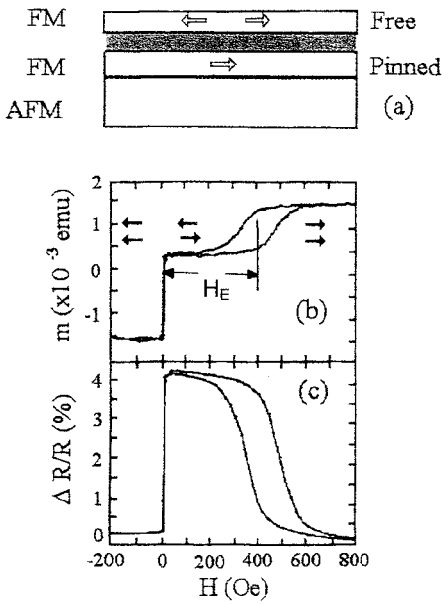

Figure 2. (a) A schematic diagram of a spin-valve device. (b) The hysteresis loop $m(H)$ and (c) magnetoresistance, $\Delta R/R(H)$, of a 6 nm $Fe_{20}Ni_{80}$/2.2 nm Cu/4 nm $Fe_{20}Ni_{80}$/7 nm FeMn GMR spin valve at room temperature. For H_E as indicated and $t_{FM} = 4$ nm, $\mu_0 M_{FM} \approx 1$ T for permalloy, we obtain from equation (2) $\sigma_{EB} = 0.13$ mJ m^{-2} [5, 6].

can use the related interface areal energy density, which we denote by σ_{EB}, for a description of the strength of the effect. The exchange field then is given by

$$H_E = \sigma_{EB}/(\mu_0 M_{FM} t_{FM}). \tag{2}$$

Here M_{FM} and t_{FM} are the magnetization and the thickness of the ferromagnetic film, adjacent to the antiferromagnet. In table 2 some representative values for σ_{EB} are given.

Table 2. Areal energy density σ_{EB} associated with the exchange bias effect due to various antiferromagnetic materials, as well as related Néel points and blocking temperatures (mainly from reference [5]).

Antiferromagnetic material	σ_{EB} (mJ m^{-2})	Néel point T_N (°C)	Blocking temperature (°C)
$Fe_{50}Mn_{50}$ (polycrystalline annealed)	0.05–0.47	217	150
$Ni_{50}Mn_{50}$ (polycrystalline annealed)	0.16–0.46	797	497
$Pt_{50}Mn_{50}$ (polycrystalline annealed)	$\leqslant 0.32$	207	127
$Ir_{18}Mn_{82}$	0.19	417	265
NiO	0.05–0.29	252	180
CoO	0.14–0.48	20	$\leqslant 20$

3. Properties of ultrathin films: Curie point, magnetization, critical behaviour

It is clear that research on ultrathin films requires extreme care with growth properties. Therefore in the following only a few examples will be discussed, which seem to be reliable and representative [2].

As intuitively expected, there is a reduction of T_C for decreasing film thickness. Systematic investigations of this aspect for Fe films showed that there can be important differences depending on which crystallographic orientation is used. For the close-packed Fe(110) monolayer on tungsten we have $T_C = 225$ K in the uncovered case and $T_C = 282$ K for a film covered with Ag. A (100)-type monolayer on the other hand seems not to order magnetically. This is believed to be due to the fact that in such a monolayer the nearest neighbours of the corresponding bulk structure are missing. If we add the nearest neighbours we arrive at a two-monolayer (100) Fe film with $T_C = 220$ K which is close to the value 225 K for the (110)-type monolayer where we have the nearest neighbours already for the monolayer.

The behaviour of the saturation magnetization in ultrathin films, i.e. the value of their magnetization at low temperatures or moment per magnetic atom, was for a long time an open question both theoretically and experimentally. The situation changed due to the substantial progress in first-principles self-consistent band theories and to the introduction of 'conversion-electron Mössbauer spectroscopy' (CEMS), in addition to the conventional magnetometries. Today there is good evidence that magnetic moments in ultrathin films are changed slightly—mostly enhanced—but this depends also on an adjacent nonmagnetic material. For example in reference [3] an increase of the Fe moment from $\mu = 2.2\ \mu_B$ as measured in the bulk to $\mu = 2.5\ \mu_B$ for a monolayer of Fe embedded in Au is reported.

For the properties of ultrathin magnetic films, the critical behaviour close to the Curie temperature T_C is also of great interest. It is related to the model by means of which we can describe the magnetic structure and the interactions which are responsible for the magnetic order. The main question is that of where, upon lowering the film thickness, 3D-type correlations change to 2D-type ones.

Just below the Curie temperature, in the range of the onset of magnetic order, the magnetization M is given by $M \propto (1 - T/T_C)^{-\beta}$ where β is a so-called critical exponent.

The value of β depends on the underlying model. It can be determined experimentally from careful measurement of M close to T_C and compared with the theory.

For thin films of Ni it was found that the crossover from 3D to 2D behaviour occurs at a thickness around 6 ML [7]. The corresponding values of T_C are around 450 K which is close to 70% of the value $T_C = 630$ K for bulk Ni. For bulk Fe and Co the Curie points are at 1043 K and 1388 K respectively. Hence the T_C-values corresponding to the crossover region are expected to be above 700 K. If one were to do such an experiment, one would have to deal with the problem of interdiffusion between film and substrate or clustering of the film material. This is why the transition region for the critical exponents has so far only been determined for thin Ni films.

4. Interlayer exchange coupling (IEC)

Ferromagnetic films can couple across nonmagnetic interlayers in various ways. When the lateral dimensions are sufficiently small, magnetostatic coupling aligning the magnetizations antiparallel can be due to flux closure at the edges. Effective ferromagnetic interlayer coupling, on the other hand, trying to align the magnetizations parallel, can occur as a result of dipolar fields produced by interface corrugations. This 'orange-peel-type' or 'Néel-type' coupling has probably been observed in many cases, although it is generally difficult to trace the origin of ferromagnetic-type coupling, because there is always also the possibility that it is due to pinholes and ferromagnetic bridges. Coupling which is due to electronic effects was first identified in 1986 for Dy and Gd films separated by Y interlayers and for Fe films separated by Cr interlayers [8]. In 1990 its oscillatory nature was recognized as a general phenomenon.

Experiments showed that IEC of ferromagnetic 3d metals across interlayers can be described phenomenologically by the connected areal energy density σ_{IEC}, via

$$\sigma_{IEC} = -J_1 \cos\theta - J_2(\cos\theta)^2. \tag{3}$$

Here θ is the angle between the magnetizations of the films on either side of the spacer layer. The parameters J_1 and J_2 describe the type and the strength of the coupling; typical values are given in table 3. If the term in J_1 dominates, then from the minima of equation (3) the coupling is ferromagnetic (antiferromagnetic) for positive (negative) J_1. If the term in J_2 dominates and is negative, we obtain 90° coupling. The first term of equation (3) is often called bilinear coupling and the second biquadratic coupling.

Table 3. A selection of observed coupling strengths and periods, collected from the literature [8].

Sample	Maximum strength J_1 in mJ m^{-2} at (thickness) in nm	Periods in ML and (nm)
Co/Cu/Co(100)	0.4 (1.2)	2.6 (0.47), 8 (1.45)
Co/Cu/Co(110)	0.7 (0.85)	9.8 (1.25)
Co/Cu/Co(111)	1.1 (0.85)	5.5 (1.15)
Fe/Au/Fe(100)	0.85 (0.82)	2.5 (0.51), 8.6 (1.75)
Fe/Cr/Fe(100)	> 1.5 (1.3)	2.1 (0.3), 12 (1.73)
Fe/Mn/Fe(100)	0.14 (1.32)	2 (0.33)
Co/Ru(0001)	6 (0.6)	5.1 (1.1)
Co/Rh/Co(111)	34 (0.48)	2.7 (0.6)
Co/Os(111-textured)	0.55 (0.9)	7 (1.5)
Co/Ir(111)	2.05 (0.5)	4.5 (1.0)

Biquadratic coupling is thought to be mainly due to interface roughness and will not be considered further here. Bilinear coupling on the other hand is believed to be due to

an indirect exchange interaction mediated by the conduction electrons of the spacer layer. It is closely related to the Ruderman–Kittel–Kasuya–Yoshida (RKKY) interaction between localized moments mediated by the conduction electrons of a host metal. However, one must consider the itinerant nature of electrons in transition metal ferromagnets which gives rise to the spin-split band structure and spin-dependent reflectivities at the paramagnet/ferromagnet interfaces.

The spin-dependent reflectivity is illustrated in figure 3(a), where it is assumed that electrons with their spins parallel (antiparallel) to the local magnetization are weakly (strongly) reflected at the interfaces. The reason for this behaviour is seen in figure 3(b). For the spin-up electrons there is a good match of the states in the ferromagnet and the interlayer as indicated by them having the same position on the energy scale. The spin-down bands in the ferromagnet show the usual upshift; therefore the good match with bands in the interlayer is now lost.

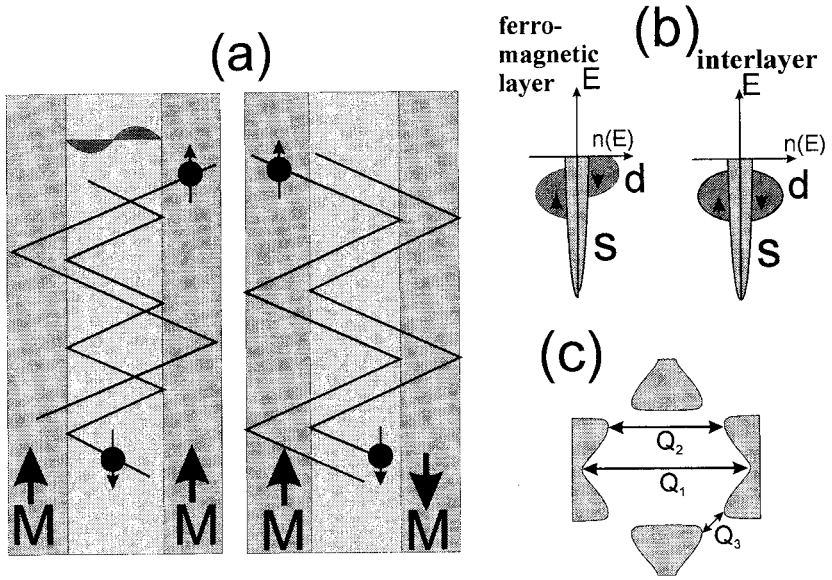

Figure 3. (a) An illustration of spin-dependent reflectivity at the nonmagnetic/magnetic interfaces used to explain oscillatory coupling. (b) Typical band structures, which are the reason for the spin-dependent reflectivity at the interfaces. (c) A cross section of the Au Fermi surface with critical spanning vectors in the [100] and [111] directions.

For the spin-down electrons this gives rise to quantum well states. As a result there are spin-dependent interference effects like the formation of standing electron waves for certain interlayer thicknesses as indicated upper left in figure 3(a). Due to the similarity of the arrangement in figure 3(a) to an optical Fabry–Perot interferometer, this is sometimes also called the Fabry–Perot model of oscillatory coupling. In the same way as the transmission of an optical Fabry–Perot interferometer for given wavelength of light oscillates as a function of the mirror distance, here the coupling oscillates as a function of the interlayer thickness. A more detailed theoretical treatment is given in e.g. reference [9].

The predominant contribution to the coupling is from electrons with wavevectors Q_i, which are critical spanning vectors of the Fermi surface of the interlayer material, i.e., vectors in the direction perpendicular to the interface that connect two sheets of the Fermi surface parallel to each other. For the Fermi surface of Au shown in figure 3(c), there are two such vectors, Q_1 and Q_2, in the [100] direction and one vector, Q_3, in the [111] direction. The

periods of the oscillatory coupling are given by $\Lambda = 2\pi/Q_i$ and thus are determined solely by the electronic properties of the interlayer material.

The experiment related to figure 3 is seen in figure 4. Part (a) shows the result of an evaluation of remagnetization curves for a Fe/Au_{wedge}/Fe structure grown on a Ag-buffered GaAs(100) substrate. The coupling is strongly ferromagnetic in figure 4(a) for small d_{Au}, probably due to pinholes and magnetic bridges. For increasing d_{Au}, the ferromagnetic coupling quickly decreases, until there are oscillations around zero. Two periods of oscillation are superimposed, with an amplitude that is attenuated as a function of the interlayer thickness.

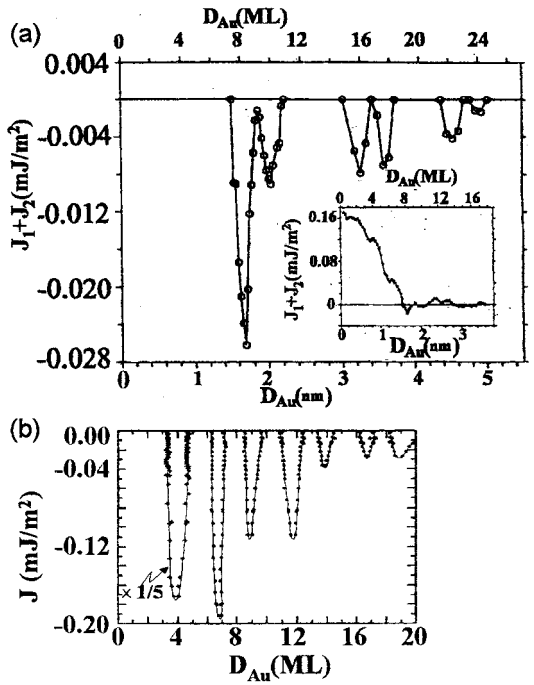

Figure 4. Coupling strength as a function of Au interlayer thickness in an Fe/Au_{wedge}/Fe (a) on an Ag-buffered GaAs substrate and (b) on an Fe whisker. The inset in (a) includes ranges where the coupling is ferromagnetic [8].

Measurements of the coupling strength in an Fe/Au_{wedge}/Fe trilayer grown on an Fe whisker, by observing the disappearance of antiferromagnetically coupled domains in a Kerr microscope, are shown in figure 4(b). Two periods of oscillatory coupling, 2.48 ML and 8.6 ML, were determined from the data. The samples used in figures 4(a) and 4(b) were both grown very carefully; the stronger coupling for the Fe whisker sample is indicative of the better growth occurring naturally on that substrate. The data of figure 4(b) were further analysed, taking into account thickness fluctuations to obtain 'unaveraged' values to compare with theory; the coupling strengths for the short- and long-period oscillations were found to be 60% and 15% of those calculated respectively.

The strength of the coupling depends on many details of the participating Fermi surfaces. It is now believed that materials from the same column of the periodic table should yield particularly large coupling strengths. This can be explained on the basis of favourable band matching [9]. The record value found for the Co/Rh combination (see table 3) seems to support this concept.

5. Giant magnetoresistance (GMR)

GMR describes the finding that in layered magnetic structures the resistivity, both for currents parallel and for currents perpendicular to the sample plane, has been found to depend on the relative magnetic alignment of adjacent ferromagnetic films on either side of an interlayer [10]. The first experiments are displayed in figure 5. For the normal effect the resistivity is highest for anti-alignment, but there can also be an 'inverse effect', where this is reversed. The AF alignment can be provided by AF interlayer exchange or e.g. by hysteresis effects. In the latter case one film is mostly magnetically pinned whereas the magnetization of the other is free to rotate in response to the external field. Such arrangements are called spin valves. Part (c) of figure 2 shows the GMR of the spin valve displayed in part (a).

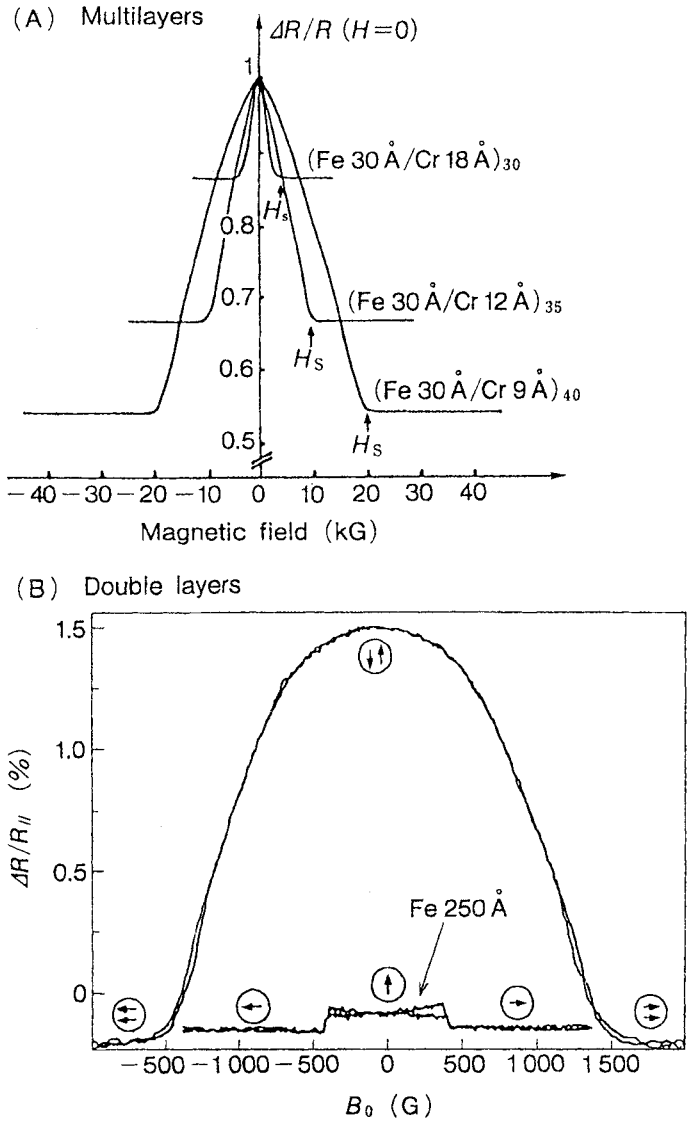

Figure 5. The first observations of the GMR effect in (A) multilayers and (B) trilayers [10].

If we denote by R_P the resistance for parallel alignment of neighbouring films and by R_{AP} that for antiparallel alignment, then the strength of the GMR is usually quoted in terms of

$$\Delta R/R_P = (R_{AP} - R_P)/R_P \ (\%). \tag{4}$$

The GMR effect has been investigated in two different geometries, namely the 'CIP' (current-in-plane) and the 'CPP' (current-perpendicular-to-plane) geometries. The relative effect is stronger in the CPP geometry, but without special structuring, due to the extremely unfavourable geometrical conditions (lateral dimensions some orders of magnitude larger than the film thickness), the voltage drop perpendicular to the layers in the CPP geometry is very difficult to detect. On the other hand, by means of structuring, the GMR in the CPP geometry can be made sufficiently strong to be of interest even for applications (see the last section). Representative and record values for the GMR effect as defined by equation (4) in the CIP and in the CPP geometry have been compiled from the literature in table 4.

Table 4. GMR: values for $\Delta R/R_\parallel$ as collected from the literature [11], which are representative of particularly strong effects or those used in sensors. The geometry is CIP unless specifically marked with CPP. AAF stands for 'artificial antiferromagnet'.

Sample	$\Delta R/R_\parallel$ (%)	Temperature (K)
$[Fe(4.5)/Cr(12)]_{50}$	220	1.5
	42	300
$[Co(15)/Cu(9)]_{30}$	78	4.2
	48	300
$[Co(8)/Cu(8.3)]_{60}$	115	4.2
	65	300
$[Co(10)/Cu(10)]_{100}$	80	300
Co(25)/Cu(19)/Co(4)/Cu(19)/Co(25)	23.4	300
Co(3)/Cu(19)/Co(25)	17	300
$Co_{90}Fe_{10}(40)/Cu(25)/Co_{90}Fe_{10}(8)\cdots$	7	300
NiFe(100)/Cu(25)/Co(22)	4.6	300
$[CoNiFe/Cu]_{4-6}$	10–20	300
Fe(60)Co(8)/Cu(23)/AAF/Cu(23)/Co(8)Fe(60)	6	300
$[Co(15)/Cu(12)]_n$, CPP	170	4.2
$[Co(12)/Cu(11)]_{180}$, CPP	55	300

The mechanism leading to GMR can be understood within Mott's two-current model. Due to their Fermi velocity, conduction electrons propagate with high speed but arbitrary direction through the layered structure, where the current is given by the drift velocity in the direction of the applied electric field. In figure 6 paths between two reflections at outer surfaces are shown, with scattering events in between. In order not to confuse the picture, the changes in direction due to the scattering events are suppressed. The scattering processes are the cause of the electric resistivity. In order to demonstrate how spin-dependent scattering leads to the GMR effect, we consider in the following a simple—albeit unrealistic—situation, where the main argument is still valid in reality.

In figure 6 it is assumed that only electrons with spin antiparallel to the local magnetization are scattered at the magnetic/nonmagnetic interfaces. Due to this condition, for parallel magnetization alignment, electrons of one type are not scattered at all, leading to a short circuit of the associated current, i.e. vanishing resistivity for the total current also. For antiparallel magnetization alignment, there are scattering events for both electrons, and hence finite resistivity for the total current. It is clear that even if the above strict condition is relaxed,

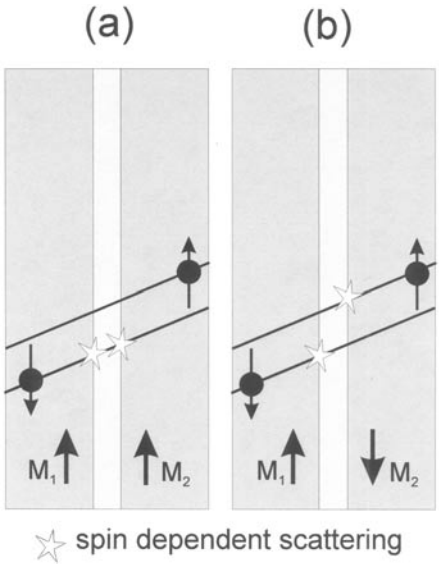

Figure 6. A simplified view of spin-dependent scattering used to explain the GMR effect. Only electrons with spin locally antiparallel to the magnetization are scattered, causing a short-circuit effect for the spin-up electrons in (a), which has disappeared in (b).

the resistivity can be higher for antiparallel magnetization alignment as compared to parallel alignment. The increase of the GMR in multilayers as compared to double layers apparent from the values in table 4 can be explained on the basis of an increased spin-dependent scattering probability when the electron has to pass many interfaces instead of only two as in figure 6.

For appropriate material combinations—in particular in the case of low-resistivity interlayers like in Co/Cu/Co structures—the GMR can also be explained by an alternative model on the basis of interface reflectivity as also seen in part (a) of figure 3. This is mainly due to the fact that for parallel magnetization alignment, due to interface reflectivity there can be an electron channelling effect in the interlayer. If the interlayer material has low resistivity, then there can be an overall low resistance. It disappears for antiparallel magnetization alignment, because spin-down as well as spin-up electrons penetrate both the ferromagnetic materials as well as the interlayers and thus the 'quasi-short-circuit effect' due to channelling in the interlayer disappears.

From the discussion of figure 6 we see that it should be possible to increase GMR ratios in trilayers by improving the specular reflectivity for the electrons at the outer surfaces, because under these conditions a double layer should be equivalent to a multilayer. A method for smoothing the outer surfaces and thus increasing the specular reflectivity has been shown to be possible; it is based on oxidation. It exploits the fact that the oxidation of a rough transition metal surface removes preferentially bumps and spikes which are converted to the insulating oxide. Hence the surface of the conducting part of the material becomes smoother. As a result of the increased specular reflectivity, record GMR values for single spin valves of 19% have been achieved [12].

Since the GMR effect in structures with Co and therefore very likely also with Co-rich alloys has been identified as mainly due to interface scattering, as illustrated in figure 6, a further increase of the GMR ratio might be expected from proper interface dusting. However, except for extremely thin Co films deposited at $Ni_{80}Fe_{20}$/Cu interfaces, which increased the

GMR ratio appreciably and showed that we are dealing here with an interface effect, not very much improvement has so far been obtained experimentally by dusting. On the other hand, since in theory such an increase is expected, the whole issue remains rather open.

6. Tunnel magnetoresistance (TMR)

The basic TMR configuration consists of two ferromagnetic electrodes—here in the form of thin films—separated by an insulating or semiconducting barrier as shown in the upper part of figure 7. The tunnel resistance depends on the relative orientation of the magnetizations on either side of the barrier [13]. Like in the case of GMR, we denote by R_P the resistance for parallel magnetization alignment and by R_{AP} that for antiparallel alignment and define TMR in the same way as GMR, by means of equation (4).

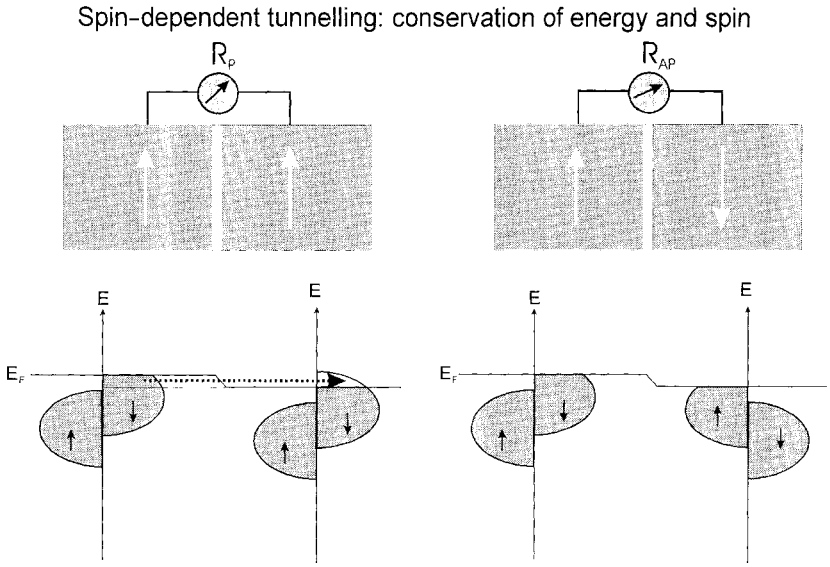

Figure 7. Spin-dependent tunnelling, as used to explain the tunnel magnetoresistance effect. Under the condition of conservation of energy and spin, and simplified band structures of 3d metals as shown, only tunnelling from occupied to empty states is possible, as indicated by the dotted arrow, i.e. for parallel alignment of the magnetizations.

Usually ΔR is positive; this is called the normal TMR effect. For the inverse effect, which can occur in special cases when different magnetic materials are used on either side of the interlayer, ΔR is negative. An example will be discussed below.

Phenomenologically, the TMR effect is treated using the relation

$$\Delta R/R = 2P_1P_2/(1 + P_1P_2). \tag{5}$$

Here P_1 and P_2 are the electron spin polarizations of the two electrodes. There is controversy as regards how to obtain the relevant values for P_1 and P_2. Most likely only the polarizations right at the interfaces are important, but certainly the spin-dependent transition probability which is determined by the material of the barrier also has to be taken into account. Figure 8 displays TMR curves which are representative for the current state of the art. Record values of around 50% have been obtained at room temperature [13, 14].

The TMR effect usually decreases as a function of the bias temperature, the origin of which is so far not clear. Spin scattering in the interlayers as well as the excitation of spin waves have

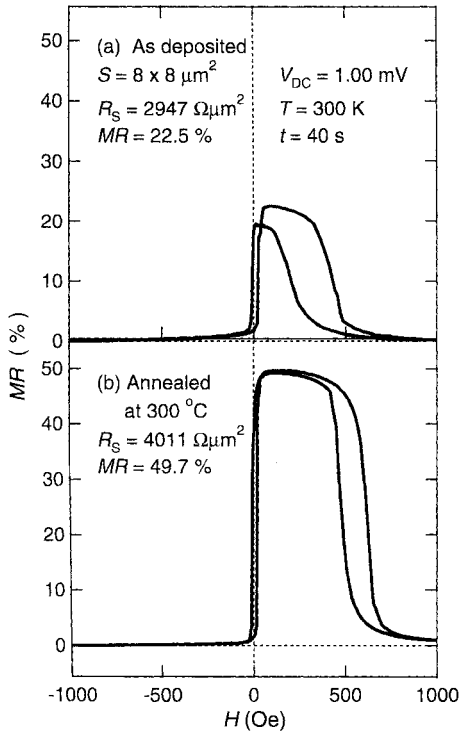

Figure 8. TMR curves measured at room temperature for films of $Co_{75}Fe_{25}$ (4 nm) across barriers of Al_2O_3 (0.8 nm). S = sample area, R_s = resistance for parallel magnetization alignment, V_{DC} = bias voltage [14].

been invoked. On the other hand, figure 9 shows an example where a bias dependence due to the shifting of the bands by the applied voltage has been observed [15]. This is revealed by the fact that the effect changes between normal and inverse as a function of the bias, which is explained in the example of figure 9 by the particular shape of the band structures and their shifts caused by the bias.

In equation (5) whether the effect is a normal or inverse one is related to whether the spin polarizations at the two interfaces have the same or opposite signs. Hence if a reference system with known sign of the polarization is used at one interface, the sign of the polarization at the other interface can be determined. de Teresa *et al* [16] used as a reference system $La_{0.7}Sr_{0.3}MnO_3$, which is known both from theory and from photoemission experiments at low temperatures to have positive spin polarization. With this system, they confirmed that the effective spin polarization at the Co/Al_2O_3 interface is positive, as found before for F/I/S junctions where: F is the ferromagnetic metal—here Co; I denotes the insulating barrier; and S is a superconductor. (F/I/S experiments had for a long time been the standard method for determining the absolute value of the relevant polarization at F/I interfaces.) A positive polarization at E_F for Co contradicts the assumption that it can be predicted from the spin-split density of states of the bulk material, which would yield negative polarization. On the other hand, it was found that the effective spin polarization of Co is negative for the $Co/SrTiO_3$ and $Co/Ce_{0.69}La_{0.31}O_{1.845}$ interfaces, which shows that it depends also on the barrier material. In summary, it is now believed that spin polarizations are related to interface states, which also play a major role in chemical bonding at the interfaces.

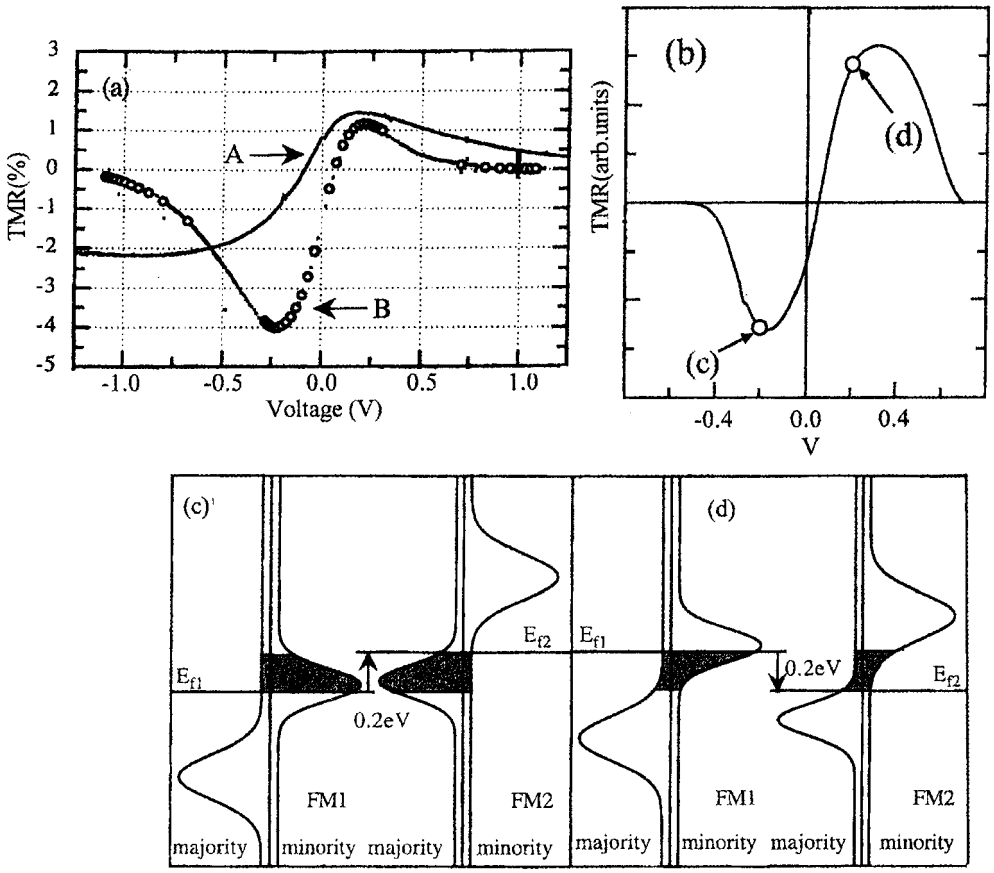

Figure 9. (a) Experimental results for TMR of permalloy films across Ta_2O_3/Al_2O_3 barriers as a function of bias voltage. (b) A simulation of the TMR curve using the band structures shown in (c) and (d), considering their relative shifts due to bias voltage. The situations shown in (c) and (d) correspond to −0.2 V and +0.2 V respectively and are specially marked in (b) [15].

The states relevant for TMR are obviously evanescent. There is an interesting connection here with the phenomenon of interlayer exchange coupling across insulating or semiconducting interlayers. From theory, it should be exponentially attenuated as a function of the interlayer thickness where the attenuation length is determined by the band gap [9]. So far it is not clear whether coupling for example across Si behaves according to this prediction or whether it is oscillatory (with the second oscillation not yet being observed experimentally) due to half-metallic silicide formation.

7. Interlayer coupling due to spin injection

The occurrence of spin-dependent reflectivity as discussed before in the context of 'interlayer exchange coupling' and 'GMR due to channelling in the interlayer' enables a further effect, namely interlayer coupling due to spin injection [17]. The experiment has been stimulated by a theory of Slonczewski [18]. An extended theoretical treatment has recently been given by Heide *et al* [19].

The experimental arrangement is displayed in figure 10(a) [17]. The sample consists of a column of layers of various materials stacked on top of each other as shown. A current can be fed in by leads I−, I+; the voltage drop is measured at V− and V+. There is a thin Co layer, Co 1, with a thickness of approximately 2.5 nm and a thick layer, Co 2, of thickness around 25 nm. The lateral diameter is around 100 nm. At negative bias, electrons flow from the thick into the thin layer and stabilize parallel magnetization alignment. At positive bias, parallel alignment is destabilized and at sufficiently large current Co 1 switches into anti-alignment.

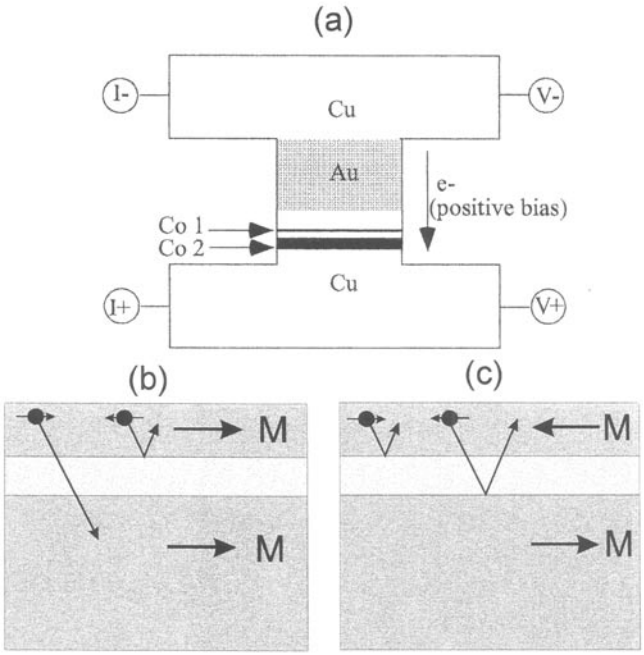

Figure 10. (a) A schematic diagram of a pillar device with Co layers separated by a 60 Å Cu layer (from reference [17]). At positive bias, electrons flow from the thin Co 1 to the thick Co 2 layer. Under these conditions, for large enough current the Co 1 layer switches into antiparallel alignment. For negative bias, parallel alignment is obtained. A possible mechanism, based on spin-dependent reflectivity, proposed here, is illustrated in parts (b) and (c). Although the complete reflections and transmissions as shown are not realistic, the main argument would hold also in reality.

The effect can be understood on the basis of spin-dependent reflectivity as already discussed in the context of figure 3(a). We use again the 'tutorial' assumption of ideal reflectivity. When the current flows from the thick to the thin layer, spin-down electrons are reflected and return to the thick layer. They act to turn the magnetization in the thick layer around. However, since this layer is thick enough, the returning electrons have only a minor effect on the total electronic balance and the thick layer does not switch.

When the current flows from the thin into the thick layer, the thin layer does switch by this mechanism, because now the returning spin-down electrons put the magnetization in the thin layer out of balance. This is displayed in figure 10(b). After the switch, the overall transfer of electrons from the thin into the thick layer is unpolarized because the two interfaces to be traversed by the electrons have opposite effects on their spin polarizations, as seen in figure 10(c). Hence there is no remaining torque. The reason for the spin-dependent reflectivity is essentially the spin splitting of the bands in the ferromagnet, as discussed in the context of figure 3.

8. Applications

Layered magnetic structures are mainly useful as storage media and as sensors in data storage technology as can be seen from the following timetable [11]:

- *1955* Proposal to use patches of permalloy films for magnetic random-access memories (MRAMs) in computers. This failed at that time because of the appearance of 'dynamic random-access memories' (DRAMs), based on semiconductors.
- *1958* Proposal to use thin films of MnBi for magneto-optic recording.
- *1973* Introduction of rare earth–transition metal (RE–TM) films for magneto-optic recording (still in use today).
- *1979* IBM introduces thin-film technology for heads in hard disks. (Both the write and the read process were still inductive, but the coil was made by thin-film technology.)
- *1991* Introduction of the anisotropic magnetoresistance (AMR) effect, using permalloy films, for sensors in hard-disk drives (HDD) by IBM.
- *1997* Introduction of GMR for the sensors in HDD, by IBM.

Other possible applications lie in robotics and sensors for controlling mechanical movements, e.g. in cars. In these sensors, IEC has also found an application, where it is exploited in 'artificial antiferromagnets (AAF)'. The miniaturization aspect and the sensitivity of GMR are also of interest for galvanic separation in signal processing, which so far has been the domain of optocouplers. Instead of converting an electrical signal into an optical one, one can use directly the fields produced by the currents together with GMR-type sensors and realize galvanic separation by means of magnetocouplers. Furthermore, GMR in conjunction with magnetostrictive materials can also be used for pressure sensors. Currently both GMR and TMR are being considered for applications in sensors and in MRAMs.

9. Final remarks

Research on magnetic film structures has contributed to a better understanding of interactions in magnetism and magnetotransport. Most effects have found interesting applications. The preparation of these structures has also had a strong impact on studies of growth and structure. The most celebrated result in this context is probably that from the study of oscillatory coupling across Cr using as substrate the almost perfect surface of an Fe whisker [8]. Under these conditions it was possible to fabricate for the first time Cr interlayers which support the incommensurate spin-density wave (ISDW), typical for almost perfect Cr. It is well known that the ISDW is extremely sensitive to imperfections. It remains a challenge to produce films of similar quality on conventional, readily available, substrates. Apart from improvements in the growth, lateral structuring has promising aspects. The experiment described in section 7 provides a recent example.

References

[1] Kundt A 1884 *Wiedemann's Ann.* **23** 228
[2] Gradmann U 1993 *Handbook of Magnetic Materials* vol 7, ed K H J Buschow (Amsterdam: Elsevier)
Elmers H J 1995 *Int. J. Mod. Phys.* **9** 3115
Daalderop G H O *et al* 1994 *Ultrathin Magnetic Structures I* ed J A C Bland and B Heinrich (Berlin: Springer)
de Jonge W J M *et al* 1994 *Ultrathin Magnetic Structures I* ed J A C Bland and B Heinrich (Berlin: Springer)
[3] Mitani S, Takanashi K, Nakajima H, Sato K, Schreiber R, Grünberg P and Fujimori H 1996 *J. Magn. Magn. Mater.* **156** 7
[4] Weber W *et al* 1996 *Phys. Rev. Lett.* **18** 3424

[5] Nogues J and Schuller I 1999 *J. Magn. Magn. Mater.* **192** 203
Berkowitz A E and Takano K 1999 *J. Magn. Magn. Mater.* **200** 552
[6] Dieny B 1994 *J. Magn. Magn. Mater.* **136** 335
[7] Li Yi and Baberschke K 1992 *Phys. Rev. Lett.* **68** 1208
[8] Bürgler D, Demokritov S O, Grünberg P and Johnson M T 2001 *Handbook of Magnetic Materials* vol 13, ed K H J Buschow (Amsterdam: Elsevier) p 3
Grünberg P and Pierce D 2001 *Encyclopedia of Materials: Science and Technology* (Amsterdam: Elsevier) at press
[9] Mathon J, Villeret M, Edwards D M and Muniz R B 1993 *J. Magn. Magn. Mater.* **121** 242
Bruno P 1995 *Phys. Rev.* B **52** 411
Stiles M 1999 *J. Magn. Magn. Mater.* **200** 322
[10] Levy P M 1994 *Solid State Physics* vol 47 (New York: Academic) p 367
Fert A, Grünberg P, Barthelemy A, Petroff F and Zinn W 1995 *J. Magn. Magn. Mater.* **140–144** 1
Barthelemy A, Fert A and Petroff F 1999 *Handbook of Magnetic Materials* vol 12, ed K H J Buschow (Amsterdam: Elsevier) pp 1–98
Fert A 2001 *Encyclopedia of Materials: Science and Technology* (Amsterdam: Elsevier) at press
Gijs M A M and Bauer G E W 1997 *Adv. Phys.* **46** 285
[11] Grünberg P 2001 *Proc. EMSA 2000; Sensors Actuators* A **91** 153
[12] Egelhoff W F *et al* 1996 *J. Appl. Phys.* **79** 8603
Egelhoff W F *et al* 1997 *J. Appl. Phys.* **82** 6142
[13] See the contributions of
Moodera J, Miyazaki T and Parkin S S P 2001 *Proc. ICM2000 (Brazil); J. Magn. Magn. Mater.* at press
[14] Han X F, Daibou T, Kamijo M, Yaoita K, Kubota H, Ando Y and Miyazaki T 2000 *Japan. J. Appl. Phys.* **39** L439
[15] Sharma M, Wang S X and Nickel J H 1999 *Phys. Rev. Lett.* **82** 616
[16] de Teresa J M, Barthelemy A, Fert A, Contour J P and Montaign F 1999 *Science* **286** 507
[17] Katine J A, Albert F J, Buhrman R A, Myers C B and Ralph D C 2000 *Phys. Rev. Lett.* **84** 3149
[18] Slonczewski J C 1996 *J. Magn. Magn. Mater.* **159** L1
[19] Heide C, Zilberman P E and Elliot R J 2001 *Phys. Rev.* B **63** 064424-1